

EFFECTS OF THE LANTHANUM CONCENTRATION ON THE $(Pb_{1-x}La_x)(Zr_{0.95}Ti_{0.05})_{1-x/4}O_3$ ANTIFERROELECTRIC CERAMIC SYSTEM

INFLUENCIA DE LA CONCENTRACION DE LANTANO EN EL SISTEMA CERÁMICO ANTIFERROELÉCTRICO $(Pb_{1-x}La_x)(Zr_{0.95}Ti_{0.05})_{1-x/4}O_3$

Y. MENDEZ-GONZÁLEZ^a, A. PELÁIZ-BARRANCO^{a†}, A. PENTÓN MADRIGAL^a, J.D.S. GUERRA^b, GUO JIE^c, WANG XIUCAI^d Y TONGQING YANG^d

a) Facultad de Física-Instituto de Ciencia y Tecnología de Materiales, Universidad de La Habana. San Lázaro y L, Vedado. La Habana 10400, Cuba; pelaiz@fisica.uh.cu[†]

b) Grupo de Ferrolétricos e Materiais Multifuncionais, Instituto de Física, Universidade Federal de Uberlândia. 38400-902, Uberlândia – MG, Brazil

c) Electronic Materials Research Laboratory, Key Laboratory of the Ministry of Education, Xi'an Jiaotong University, Xi'an 710049, China

d) Functional Materials Research Laboratory, College for Materials Science and Engineering, Tongji University, 4800 Caoan, Shanghai 201804, China

† corresponding author

Recibido 14/3/2016; Aceptado 14/4/16

Lanthanum modified lead zirconate titanate antiferroelectric ceramics has been studied by using X-ray diffraction, dielectric analysis and ferroelectric hysteresis loops. Both antiferroelectric-orthorhombic (Pbam) and ferroelectric-rhombohedral (R3c) phases co-exist in the studied compositions. The dielectric response has revealed the presence of two peaks in a wide temperature range, which have been associated to different phase transitions. Slim-like hysteresis loops were obtained at room temperature, suggesting a higher stability of the antiferroelectric phase. The hysteresis and dielectric results show that the increase of the La^{3+} ions concentrations disrupts the long-range dipolar order for the ferroelectric phase.

En este trabajo han sido estudiadas cerámicas antiferroeléctricas de circonato-titanato de plomo modificadas con lantano utilizando difracción de rayos-X, mediciones dieléctricas e histéresis ferroeléctrica. Los patrones de difracción de rayos-X muestran, para todas las composiciones, la coexistencia de fases ferroeléctrica con simetría romboédrica (R3c) y antiferroeléctrica con simetría ortorrómbica (Pbam). Los resultados de la respuesta dieléctrica mostraron dos picos en su comportamiento, asociados a diferentes transiciones de fase. La dependencia P-E, a temperatura ambiente, sugiere una mayor estabilidad de la fase antiferroeléctrica. Los resultados de las propiedades dieléctricas y la histéresis ferroeléctrica muestran que el incremento de la concentración de los iones La^{3+} debilita las interacciones de largo alcance que establecen el orden ferroeléctrico.

PACS: Antiferroelectric materials, 77.84.-s; Dielectric properties permittivity, 77.22.Ch; Hysteresis in ferroelectricity, 77.80.Dj

I. INTRODUCTION

The dielectric materials are typically used to increase the energy storage in capacitors. It is also known that for practical applications, high electric breakdown field, large saturated polarization and small remanent polarization are required [1]. From this point of view, it has been considered that antiferroelectric (AFE) materials are potential candidates for electrical energy storage capacitors. These systems, which are characterized by double-like hysteresis loops, possess electric dipoles with antiparallel ordering such that no macroscopic electrical polarization can arise. In the presence of an electric field, an AFE state can be forced into a ferroelectric state, storing large amounts of electrical energy due to the sudden increase in the polarization [1]. AFE materials show interesting physical properties. In addition to their energy storage capacity; they exhibit electrocaloric effect, which is higher than in ferroelectrics and lineal dielectrics. Due to their properties, these systems are very attractive for practical applications such as dielectric capacitors, electrocaloric refrigerators, actuators and transducers [1,2]. Several studies have been performed on these materials

[1,3–10]. Lead-containing ceramics, such as lead zirconate [1,5] and modified lead zirconate titanate (PZT) [2,6–14], are considered the most important antiferroelectrics. It has been evaluated, for some systems, that doping by using La^{3+} ions generally provides the stability of the AFE phase over the ferroelectric phase [2,11–14]. The aim of present work is to evaluate the effect of the lanthanum modification on the antiferroelectric phase for $(Pb_{1-x}La_x)(Zr_{0.95}Ti_{0.05})_{1-x/4}O_3$ ($x = 0, 1, 2, 3$ and 4 at %) antiferroelectric ceramics. Samples are investigated by using structural analysis, dielectric response and hysteresis loop measurements.

II. EXPERIMENTAL PROCEDURE

Ceramics samples of $(Pb_{1-x}La_x)(Zr_{0.95}Ti_{0.05})_{1-x/4}O_3$ ($x = 0, 1, 2, 3$ and 4 in %) were prepared by the traditional solid-state reaction method [13]. High purity chemical precursors of PbO (99.9 %, Alfa Aesar), TiO_2 (99.9 %, Johnson Matthey), ZrO_2 (99 %, Merck) and La_2O_3 (99.99 %, Alfa Aesar) were used as starting powders. The mixed oxides were milled for 2 hours, dried and pressed (1 ton/cm^2). Calcination was carried out at 800°C for 1 hour in air atmosphere. The powders were

milled again for 1 hour, dried and pressed (2 ton/cm^2). The sintering was performed in a closed platinum crucible and air atmosphere at 1250°C for 1 hour. The powder samples were investigated, at room temperature, by using X-ray diffraction (XRD) experiments (Persee XD3 diffractometer, $\text{CuK}\alpha$ radiation). It was used a scan step of 0.02° for 2θ from 10° to 85° . Silver painted-electrodes were applied on the parallel faces of the disk-like samples by a heat treatment at 590°C . The temperature and frequency dependence of the dielectric constant were obtained from room temperature until 350°C , in a wide frequency range ($1 \text{ kHz} - 1 \text{ MHz}$) by using an LCR meter (IOKI 3532-50). Polarization–Electric field (P-E) hysteresis loops were obtained by using a Radiant system at 10 Hz. The samples were labeled as PLZT $x/95/5$ for the results and discussion.

III. RESULTS AND DISCUSSION

Figure 1(a) shows the X-ray diffraction patterns (XRD), at room temperature, for the studied ceramics. The indexation is the same for all compositions. It can be seen that both antiferroelectric-orthorhombic (Pbam) and ferroelectric-rhombohedral (R3c) phases co-exist. Figure 1(b) shows two typical regions for a better understanding of the contribution of both phases. An unknown peak (marked with an asterisk) has been found around 28° , for all compositions. Its origin is currently under study.

The XRD-profile analysis was carried out by using the FullProf Suit software [15], assuming the formation of both phases for the initial structural model. The refinement procedure allowed getting reasonable goodness of fit parameters and a good agreement between the observed and calculated patterns was found. Table 1 shows the unit cell parameters and the unit cell volume (V) for both phases. It can be seen that the lattice parameters depend on the La^{3+} ions concentration. The unit cell volume for the orthorhombic phase increases with the lanthanum content, while for the rhombohedral phase tends to decrease.

Table 1. Values of the unit cell parameters and the unit cell volume for both phases.

Orthorhombic phase (Pbam)	$a(\text{\AA})$	$b(\text{\AA})$	$c(\text{\AA})$	$V(\text{\AA}^3)$
PLZT 0/95/5	5.867(2)	11.745(2)	8.207(3)	565.57(6)
PLZT 1/95/5	5.865(8)	11.740(9)	8.208(5)	565.31(1)
PLZT 2/95/5	5.866(1)	11.746(1)	8.213(1)	565.88(2)
PLZT 3/95/5	5.876(5)	11.775(7)	8.224(4)	569.12(8)
PLZT 4/95/5	5.877(4)	11.777(4)	8.227(2)	569.56(9)
Rhombohedral phase (R3c)	$a(\text{\AA})$	$b(\text{\AA})$	$V(\text{\AA}^3)$	
PLZT 0/95/5	5.837(5)	14.409(9)	425.33(9)	
PLZT 1/95/5	5.840(1)	14.407(1)	425.55(4)	
PLZT 2/95/5	5.836(4)	14.418(5)	425.38(2)	
PLZT 3/95/5	5.835(2)	14.384(2)	424.16(2)	
PLZT 4/95/5	5.836(7)	14.388(0)	424.60(9)	

The temperature dependence of the real part of the dielectric permittivity (ϵ') is shown in Figure 2, for several

frequencies. It can be seen two peaks or anomalies, which could be associated to different phase transitions in the studied temperature range. The observed behavior has been previously reported for PLZT systems [14, 16–18], with an anomaly at lower temperatures (T_1) and a maximum at the temperature corresponding to ϵ'_{max} values (T_m). No frequency dependence for T_m is observed.

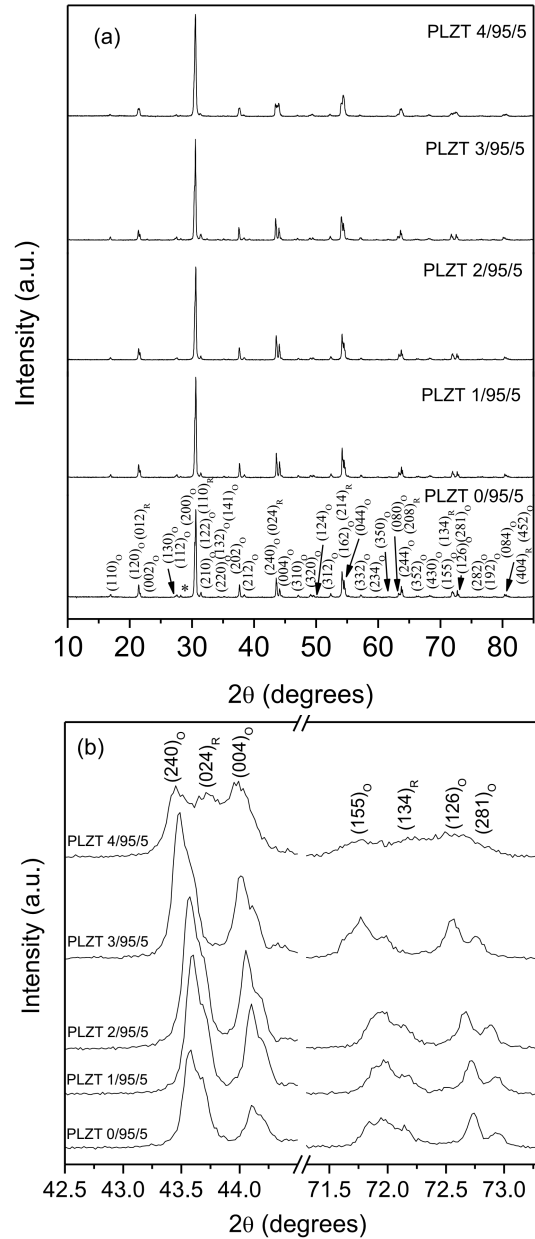


Figure 1. (a). X-ray diffraction patterns, at room temperature, for the studied ceramics; (b) zooms of two XRD pattern regions, $42.5^\circ - 44.5^\circ$ and $71.3^\circ - 73.3^\circ$.

For doping values up to 2 at%, the T_m values shifts toward lower temperatures with increasing of the La^{3+} ions concentration, reaching a minimum and then increases for higher lanthanum concentrations (see Table 2). This increase could be associated to the increasing of T_1 values for PLZT 3/95/5 and PLZT 4/95/5 or a possible incorporation of a

fraction of the rare-earth at B-sites considering that the 6-coordination ionic radius for La^{3+} is 104.5 pm , which is greater than that of the ionic radius for Ti^{4+} (61 pm) and Zr^{4+} (72 pm) [19–21]. Furthermore, a broadening in the dielectric permittivity peaks was observed with the increase of the La^{3+} content. This broadening can be attributed to various factors, such as compositional inhomogeneity, structural disorder and microstrains [22].

Table 2 shows the dielectric parameters for the studied compositions. Clear composition dependence is observed for T_1 and T_m values. With increasing of rare earth concentration, the low-temperature phase transition shows a tendency to increase.

On the other hand, the increase of the La^{3+} ions content causes a strong decreasing of ϵ'_{max} values (see Table 2). This behavior has been also noticed for PLZT $x/90/10$ [14]. It could be associated with the grain size variation when the lanthanum concentration increases [23]. Scanning Electron Microscopy measurements have showed a decrease in the grain size with the increase in rare earth content for the studied compositions. A decrease in the grain size provides an increase in the volume fraction of the grain boundaries. Then, a clamping of the domain walls at the grain boundaries from its neighbors becomes stronger, making it more difficult the orientation of the domains. The domain wall mobility will decrease, leading to a decrease in the real dielectric permittivity with the grain size.

Table 2. The dielectric parameters for the studied samples.

Samples	$T_1(^{\circ}\text{C})$	$T_m(^{\circ}\text{C})$	$\epsilon'(1\text{kHz})$	$T_{\epsilon'_{max}}(^{\circ}\text{C})$
PLZT 0/95/5	99	244	8309	244
PLZT 1/95/5	133	221	6808	221
PLZT 2/95/5	127	213	3951	213
PLZT 3/95/5	205	234	1556	232
PLZT 4/95/5	213	244	697	240

Another factor that could be inducing the ϵ'_{max} behavior is the influence of the lanthanum concentration on the dipole moment of the system. The La^{3+} ions replace the ferroactive Pb^{2+} ions. Due to the difference in charge and size between these ions, the dipole moment value is affected and thereby the polarization and the real part of the dielectric permittivity values.

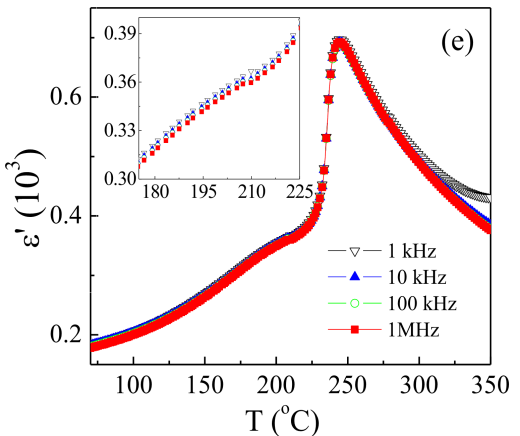
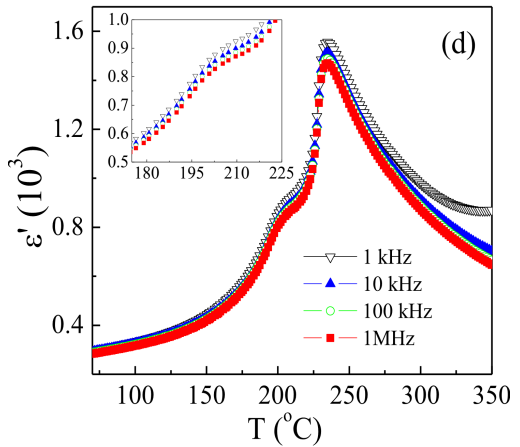
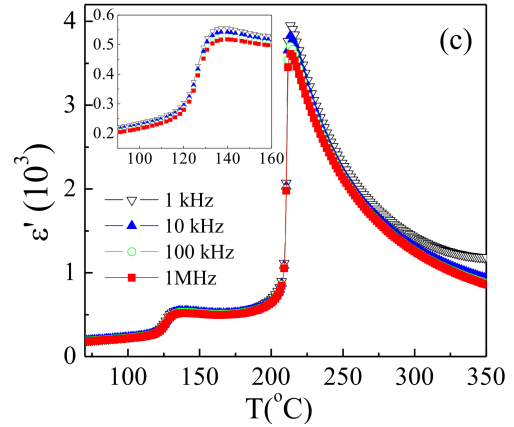
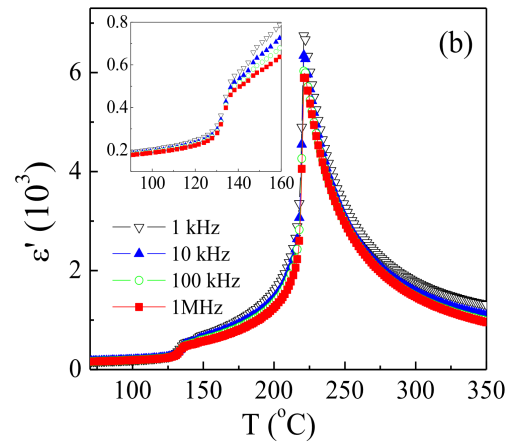
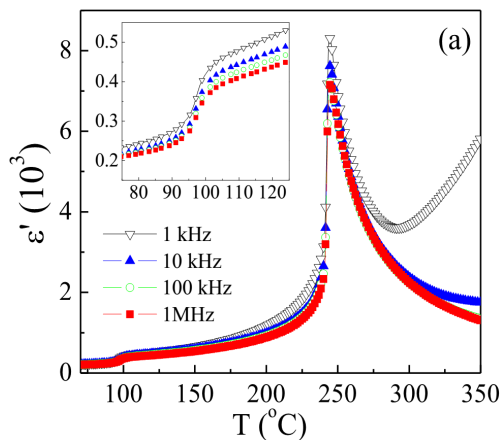


Figure 2. Temperature dependence of the real dielectric permittivity (ϵ'), at several frequencies, for (a) PLZT 0/95/5, (b) PLZT 1/95/5, (c) PLZT 2/95/5, (d) PLZT 3/95/5 and (e) PLZT 4/95/5.

Figure 3 shows the temperature dependence of the imaginary part of the dielectric permittivity (ϵ'') at several frequencies, for the studied compositions. The temperature corresponding to the maximum imaginary dielectric permittivity value ($T_{\epsilon'' \max}$) was obtained around T_m values (Table 2) and no frequency dependence was observed. The observed dielectric behavior considering both temperature and frequency dependences (Figures 2 and 3) is typical of materials showing normal behavior in the ferroelectric-paraelectric phase transition. High values of ϵ'' are also observed at the higher temperature range, especially in the low frequency range, which can be attributed to the conduction losses effects [2].

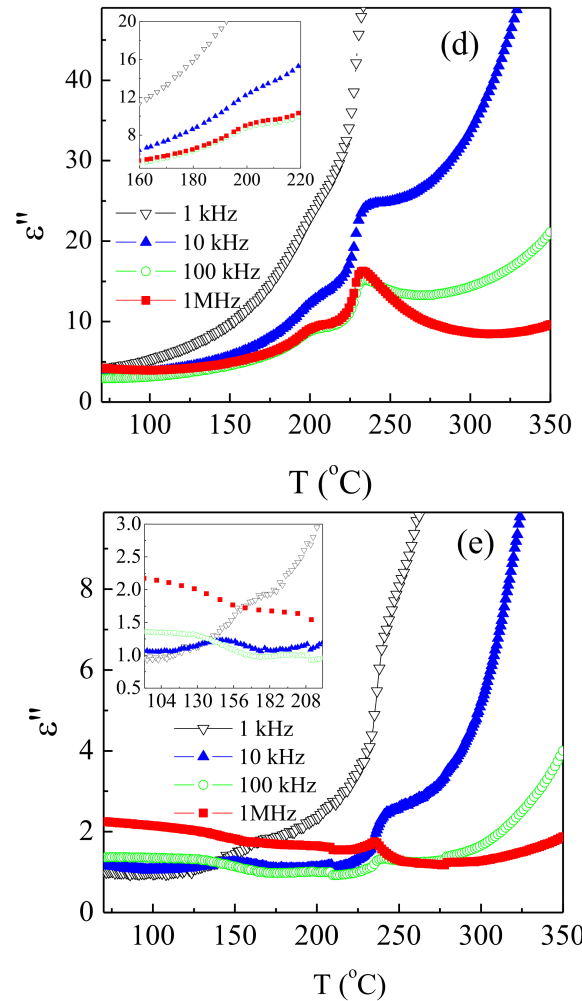
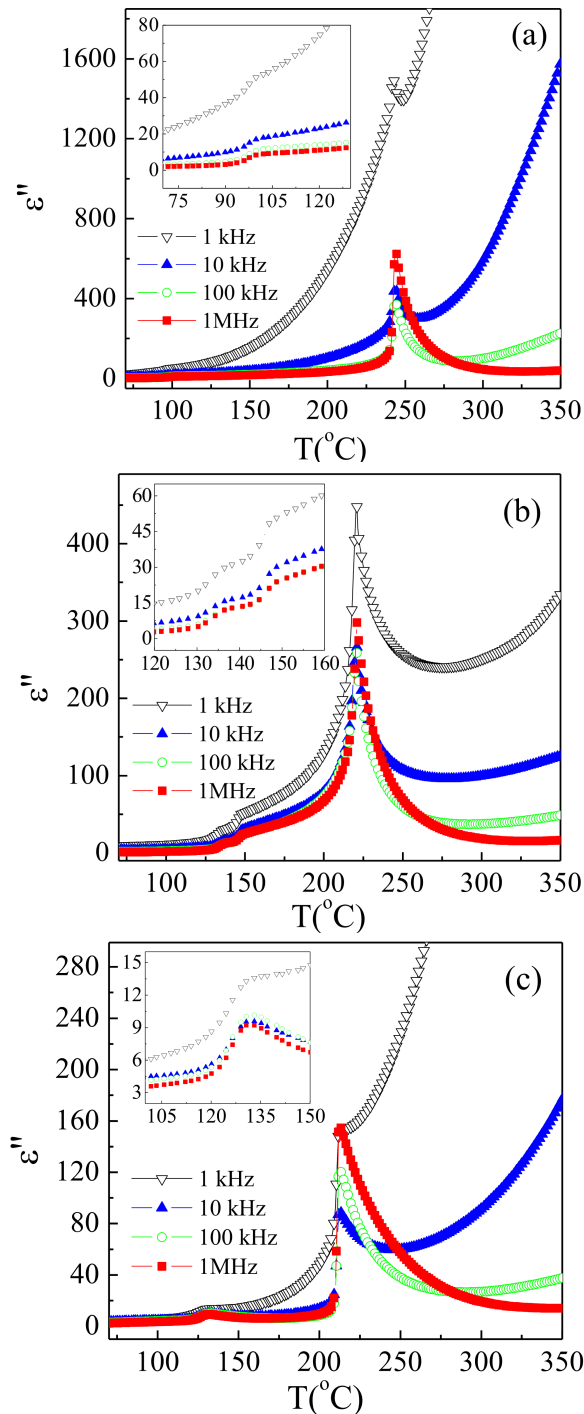


Figure 3. Temperature dependence of the imaginary dielectric permittivity (ϵ''), at several frequencies, for (a) PLZT 0/95/5, (b) PLZT 1/95/5, (c) PLZT 2/95/5, (d) PLZT 3/95/5 and (e) PLZT 4/95/5.

The hysteresis loops, at room temperature, are shown in Figure 4 for the studied compositions. The P-E dependence has revealed a double hysteresis loop for PLZT 0/95/5 (Figure 4(a)) and slim-like hysteresis loops for higher La^{3+} concentrations, suggesting an antiferroelectric character for all samples. The lanthanum concentration influences on the remanent polarization values (P_r). When the same electric field is applied on the studied samples, an increase in the La^{3+} content provides a tendency to decrease in the P_r values. This trend seems to be consistent with the observed tendency in the unit cell volume for the ferroelectric-rhombohedral phase. A contraction in its V suggests a decrease in the dipole moment and thereby in the polarization value.

The Pb–O–Zr/Ti bounding coupling in La^{3+} -doped samples plays an important role on these results [24]. Lead Pb^{2+} ions establish the long-range ferroelectric interactions in PZT systems due to the strong Pb–O–Zr/Ti bounding coupling [24]. This bounding defines the energy barrier between different polarization states (0, +P, -P), which are set by shift of $\text{Ti}^{4+}/\text{Zr}^{4+}$ ions. The Pb^{2+} substitution by La^{3+} ions weakens the bounding, causing a decrease in the energy barrier [24]. The lower is the barrier energy, the dipoles will have greater

ability of move back to their original configuration once the applied electric field is removed, and therefore, should expect lower remanent polarization in the studied samples when the lanthanum concentration increases.

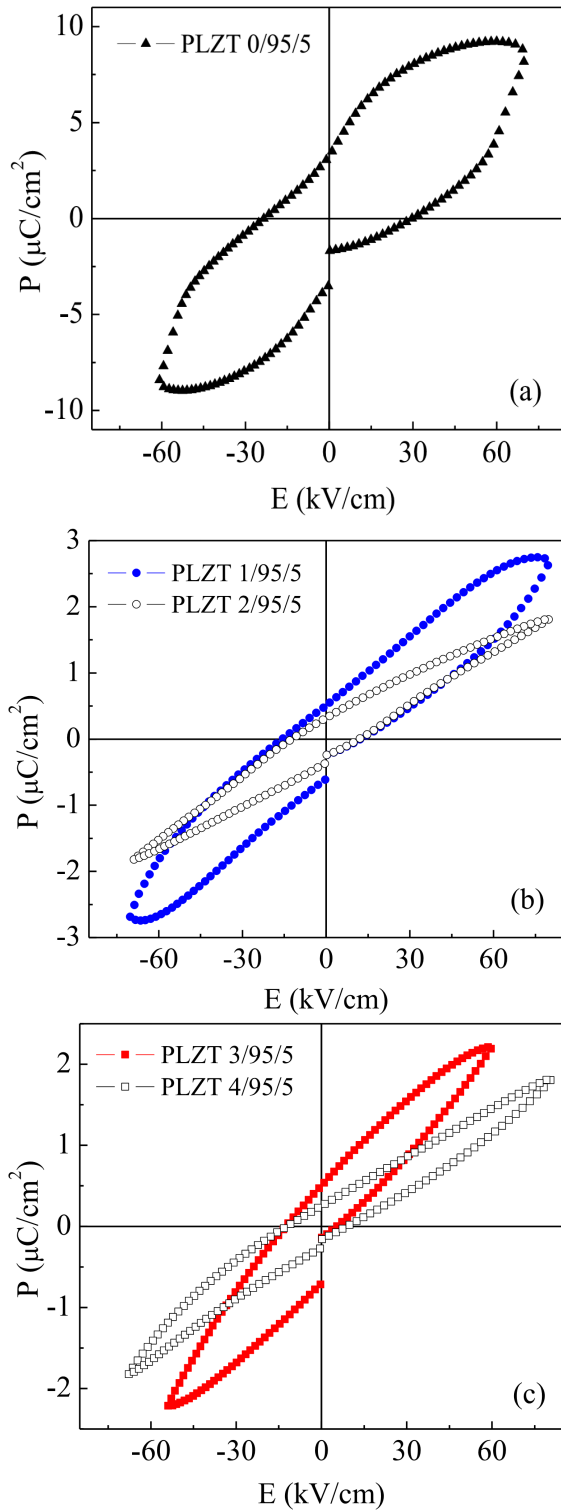


Figure 4. Hysteresis loops, at room temperature, for (a) PLZT 0/95/5, (b) PLZT 1/95/5 and PLZT 2/95/5, (c) PLZT 3/95 and PLZT 4/95/5.

In order to identify the phase transformations sequence, hysteresis measurements at several temperatures were

performed for two compositions. Figure 5 shows the P-E behavior for PLZT 1/95/5 at several temperatures. From room temperature to until around 100°C, the double-like hysteresis loops have suggested the AFE phase stability. Above that, typical ferroelectric hysteresis loops have suggested the FE phase stability, which is confirmed at 140°C by the squareness of the hysteresis loop. These results suggest that between 100 – 140°C an AFE-FE phase transition could take place. Then, the first anomaly, which has been observed in the dielectric measurements around 133°C could be associated to an AFE-FE phase transition for PLZT 1/95/5 system.

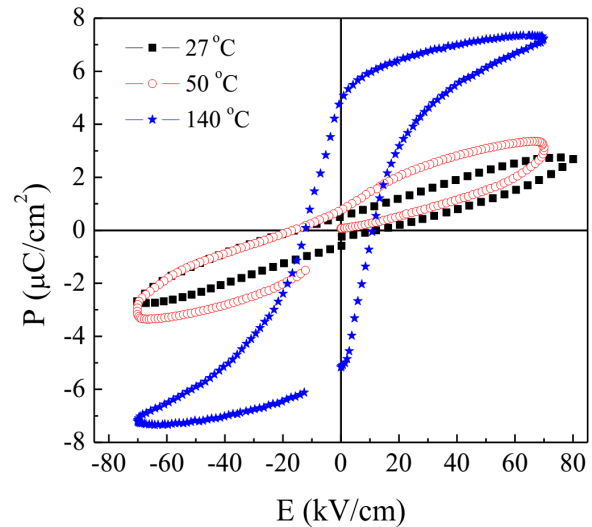


Figure 5. Hysteresis loops for PLZT 1/95/5 at several temperatures.

For PLZT 2/95/5, the results have shown a quite different behavior. Figure 6 shows the hysteresis loops at several temperatures. The results have suggested for all the studied temperature range, the AFE phase stability. Then, the first anomaly in Figure 2 cannot be associated to an AFE-FE phase transition. Previous reports on similar compositions by using transmission electron microscopy (TEM) have suggested an AFE-AFE phase transition, being the second one AFE phase an incommensurate state (AFEin) [12, 17–25].

It is known that ferroelectricity results from long-range Coulomb interactions between atomic dipole moments [13]. On the other hand, antiferroelectricity results from nearest neighbor interactions (sublattice coupling) between dipole moments. The short-range nature of the interactions can be affected for defects into structure. Consequently, the stability of the AFE state may be sensitive to small amounts of impurities. The lanthanum incorporation into PZT perovskite structure, with high Zr^{4+} concentration, provides a competition between the antiferroelectric and ferroelectric ordering, resulting in an AFEin-order around T_1 for 2 at% and higher lanthanum concentration [11, 12]. Thus, it can be considered that the lanthanum concentration favors a change in the phase transition sequence around T_1 . Moreover, an increase of the T_1 values when the La^{3+} content increases could suggest a higher temperature range for the AFE phase stability.

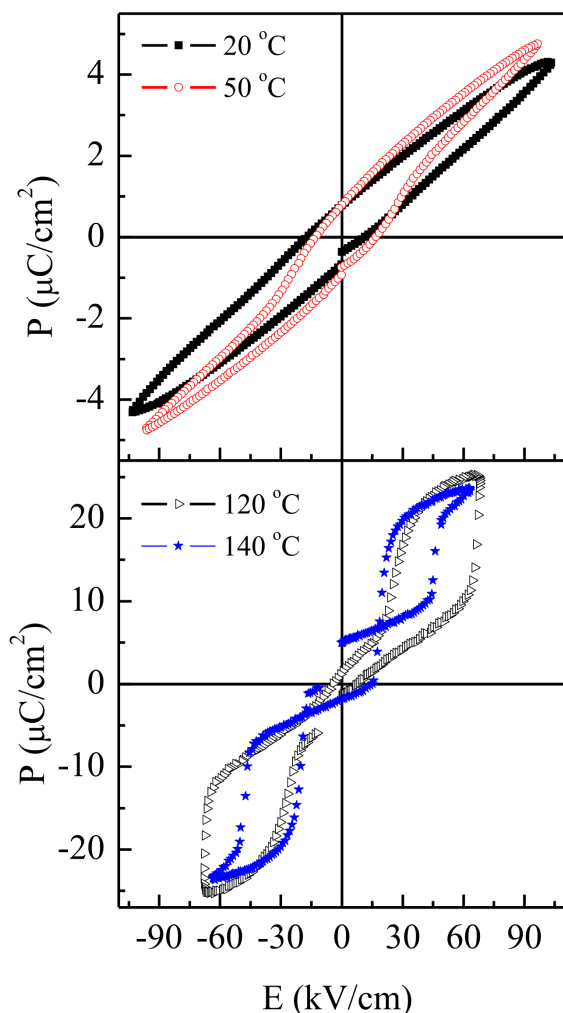


Figure 6. Hysteresis loops for PLZT 2/95/5 at various temperatures.

IV. CONCLUSIONS

Lanthanum modified lead zirconate titanate antiferroelectric ceramics have been studied to evaluate the effect of the lanthanum concentration on the antiferroelectric phase. Structural studies have revealed that both antiferroelectric-orthorhombic and ferroelectric-rhombohedral phases coexist at room temperature for the studied compositions. Dielectric measurements have showed two anomalies, which have been associated to different phase transitions in the studied temperature range. The P-E dependence, at room temperature, has suggested the antiferroelectric phase stability for all the studied samples. The analysis in a wide temperature range has suggested that the phase transition sequence depends on the lanthanum concentration.

V. ACKNOWLEDGMENTS

The authors would like to acknowledge the Third World Academy of Sciences (RG/PHYS/LA Nos. 99-050, 02-225 and 05-043), and the ICTP, Trieste-Italy, for financial support of Latin-American Network of Ferroelectric Materials

(NET-43). Thanks to CNPq (300123/2015-9, 401072/2014-2) and FAPEMIG Brazilian agencies for financial support. Dr. Peláiz-Barranco would like to thank to Tongji University (Shanghai, China) and Xi'an Jiatong University (Xi'an, China) for financial support.

REFERENCES

- [1] Hao, J. *Adv. Dielect.* 3, 1330001 (2013).
- [2] A. Peláiz-Barranco, J.D.S. Guerra, O. García-Zaldívar, F. Calderón-Piñar, M.E. Mendoza, D.A. Hall, E.B. Araújo, *Solid State Commun.* 149, 1308 (2009).
- [3] G. R. Love, *J. Am. Ceram. Soc.* 73, 323 (1990).
- [4] W. J. Sarjenat, J. Zirnheld and F. W. Macdougall, *IEEE Trans. Plasma Sci.* 26, 1368 (1998).
- [5] A. S. Mischenko, Q. Zhang, J. F. Scott, R. W. Whatmore and N. D. Mathur, *Science* 311, 1270 (2006).
- [6] H. Zhang, X. Chen, F. Cao, G. Wang, X. Dong, Z. Hu and T. Du, *J. Am. Ceram. Soc.* 93, 4015 (2010).
- [7] X. Chen, F. Cao, H. Zhang, G. Yu, G. Wang, X. Dong, Y. Gu, H. He and Y. Liu, *J. Am. Ceram. Soc.* 95, 1163 (2012).
- [8] S. E. Young, J. Y. Zhang, W. Hong and X. Tan, *J. Appl. Phys.* 113, 054101 (2013).
- [9] X. Hao, Y. Wang, L. Zhang, L. Zhang and S. An, *Appl. Phys. Lett.* 102, 163903 (2013).
- [10] A. Peláiz-Barranco, Y. González-Abreu, Jinfei Wang and Tongqing Yang, *Rev. Cub. Fis.* 31, 98 (2014).
- [11] X. Daí and D. Viehland, *J. Appl. Phys.* 76, 3701 (1994).
- [12] D. Viehland, X. H. Dai, J. F. Li and Z. Xu, *J. Appl. Phys.* 84, 458 (1998).
- [13] Y. Xu, *Ferroelectric materials and their applications* (Elsevier Science Publishers B. V., The Netherlands, 1991).
- [14] A. Peláiz-Barranco, J. D. S. Guerra, O. García-Zaldívar, F. Calderón-Piñar, E. B. Araújo, D. A. Hall, M. E. Mendoza and J. A. Eiras, *J. Mater. Sci.* 43, 6087 (2008).
- [15] J. Rodríguez-Carvajal, FULLPROF: A Program for Rietveld Refinement and Pattern Matching Analysis, Abstracts of the Satellite Meeting on Power Diffraction of the XV Congress International Union of Crystallography Toulouse, France (1990), p. 127.
- [16] Z. Ujma, J. Haiiderek, H. Hassan, G. E. Kugel and M. Pawelczyk, *J. Phys.: Condens. Matter* 7, 895 (1995).
- [17] D. Viehland, Jie-Fang Li, X. Dai, Z. Xu, *J. Phys. Chem. Solids* 57, 1545 (1996).
- [18] J. Hariderek and Z. Ujma, *J. Phys.: Condens. Matter* 7, 1721 (1995).
- [19] G. P. Espinosa, *J. Chem. Phys.* 37, 2344 (1962).
- [20] R. D. Shannon, *Acta Crystallogr. A* 32, 751 (1976).
- [21] D. R. Lide. *Handbook of Chemistry and Physics* (CRC Press, 2004).
- [22] B. P. Das, R. N. P. Choudhary and P. K. Mahapatra, *J. Mater. Sci.: Mater Electron* 20, 534 (2009).
- [23] L. B. Kong, J. Ma, R. F. Zhang and T. S. Zhang, *J. Alloys Comp.* 339, 167 (2002).
- [24] I-Wei Chen, Ping Li, Ying Wang, *J. Phys. Chem. Solids* 57, 1525 (1996).
- [25] X. Daí and D. Viehland, *J. Appl. Phys.* 65, 3287 (1994).